Universal classification scheme for the spatial-localization properties of one-particle states in finite, d-dimensional systems

János Pipek and Imre Varga
Quantum Theory Group, Institute of Physics, Technical University of Budapest, H-1521 Budapest, Hungary
(Received 4 April 1991; revised manuscript received 18 March 1992)

The spatial-localization properties of general lattice distributions (e.g., charge distribution of one-particle eigenstates) are studied. We have introduced a localization quantity, the *structural entropy* characteristic of the decay form (shape) of the distribution. We have found that there exists a nontrivial relation between the structural entropy and the well-known delocalization index (participation ratio) where the latter parameter measures the spatial extension of the distribution. This relation is universal in the sense that it is independent of the geometrical arrangement of the atomic network, of the lattice constant, and of the size of the system, and is fully determined by the decay form of the eigenstates and the dimension d of the lattice. Based on this relation we have developed a classification scheme for the characterization of the shape and extension of the one-particle states, which makes possible the identification of various decay forms (Gaussian, exponential, power law, etc.) in numerical calculations even on finite systems. The implementation of our method in already existing program systems is particularly easy. Besides presenting the theoretical background we demonstrate its applicability on some numerical calculations.

PACS number(s): 05.50.+q, 31.15.+q, 31.90.+s, 71.50.+t

I. INTRODUCTION

Recently the spatial characterization of one-particle eigenstates seems to be a common problem in diverse fields of physics. Besides the spectral properties, the localization or delocalization features and the functional decay forms of the eigenstates have also been studied intensively due to their emerging importance, especially in conductivity calculations.

The localization phenomenon induced by disorder is still in the center of interest since Anderson's original work [1]. Extensive study has been performed both analytically and numerically via a noninteracting tight-binding Hamiltonian. Several review articles [2–8] and other research reports [9–14] have already been published, from which we may learn that detecting localization in numerical calculations suffers from some unresolved difficulties. The numerical study of infinite random systems is usually performed by cluster calculations; therefore it is essential to be able to classify the eigenstates of finite systems and separate localized states from extended ones. The detailed shape analysis of the wave functions is fairly difficult. The concept of the "envelope" is mathematically ill-defined; thus the application of unique shape descriptive indices would be preferred. The aim of this work is to propose a technique that provides a fast and efficient characterization of the wave functions.

Similar questions have arisen in the study of various models; e.g., the hierarchical tight-binding model [15], the localization on fractals [16–18], quasiperiodic lattices [17,19,20], the quantum chaos of the kicked rotor and the eigenstates of band random matrices [21], and even the classical waves in a random medium [22], all of which urge a classification scheme where general one-particle eigenstates may be characterized according to their spatial extension and localization properties. In other results [23], the existence of extended states in the presence of disorder is still questioned [2–8]. The problem of two-dimensional disordered systems in magnetic fields [24,25] also shows the significance of the spatial structure of the wave functions. In this case the distinguishing of exponential and Gaussian localization may lead to significant physical consequences.

In this paper we present a method for the description of the decay form of general (charge, probability, etc.) distributions. Although the above-mentioned problems are mainly of solid-state-physics origin, the applicability of this shape analysis extends over a broad range of physical problems.

The organization of this paper is as follows. In the main text we have focused our attention on the basic physical considerations, whereas mathematical details are shown in various Appendixes. Section II contains the general formulation of the theory for discrete lattices, while Sec. III treats the connection between the decay form of the wave functions and the localization indices. Extreme delocalization and localization are discussed in Secs. IV and V, respectively. Numerical applications (random wave function, one-dimensional quasiperiodic system, planar molecules, two-dimensional disorder) will be presented in Sec. VI. The summary of the results can be found in Sec. VII.

II. DISCRETE LATTICE MODEL

We consider a general lattice of N sites in arbitrary spatial dimensions. We assume the existence of M normalized one-particle states (occupied or unoccupied), where M is not necessarily equal to N. Latin letters are

used to denote site indices and greek letters for one-particle states.

Since we would like to characterize the overall behavior of the "envelope" of the one-particle functions, it seems to be obvious to consider, instead of the wave function itself, the contribution Q_i^μ of a given site i to the state $|\mu\rangle$. In the simplest case of an orthonormal site expansion $\{|i\rangle, i=1,\ldots,N\}$, Q_i^μ are the square moduli of the expansion coefficients $|c_i^\mu|^2$. More generally these quantities can be defined as the so-called Bader charge [26] of the one-particle wave function on site i. The idea behind the latter definition is a unique subdivision of the embedding space into "atomic" regions and integrating the square modulus of the wave function over this area. For the sake of simplicity we will call Q_i^μ the "charge accumulated on site i due to orbital $|\mu\rangle$" but we wish to emphasize that it can actually be any normalized lattice distribution that satisfies the following restrictions:

$$0 \le Q_i^\mu, \quad i=1,\ldots,N, \quad \mu=1,\ldots,M , \tag{2.1a}$$

$$\sum_{i=1}^{N} Q_i^\mu = 1, \quad \mu=1,\ldots,M . \tag{2.1b}$$

If Q_i^μ means the charge distribution of wave function $|\mu\rangle$, Eq. (2.1b) is simply the normalization condition of $|\mu\rangle$.

We introduce the so-called participation ratio [27,28] or delocalization measure [29]

$$D^\mu = \left[\sum_{i=1}^{N} (Q_i^\mu)^2 \right]^{-1} . \tag{2.2}$$

This quantity has been extensively used for the characterization of eigenstates [2,10–15,19,27]. Recently exact derivations of this parameter have been given [28,29]. The participation ratio gives approximately the number of sites to which the state $|\mu\rangle$ extends. Hereafter, given an eigenstate, we will drop the index μ where it does not create any confusion. We may normalize D to the number of sites present in the system in order to get a size-independent parameter, the *spatial filling factor* of the wave function

$$q = \frac{D}{N} . \tag{2.3}$$

We have already shown in a previous publication [29] that restriction (2.1b) implies the relations

$$0 \le D \le N , \tag{2.4}$$

while from (2.1a) and (2.1b) follows

$$0 \le Q_i \le 1 , \tag{2.5a}$$

$$D^{-1} = \sum_{i=1}^{N} (Q_i)^2 \le \sum_{i=1}^{N} Q_i = 1 . \tag{2.5b}$$

Relation (2.5b) shows a further restriction on quantity D, which together with relations (2.4) gives

$$1 \le D \le N , \tag{2.6a}$$

$$1/N \le q \le 1 . \tag{2.6b}$$

For infinite systems ($N \to \infty$) q is always in the (0,1] interval, i.e.,

$$0 < q \le 1 . \tag{2.6c}$$

Besides D we will use the Shannon entropy or the information entropy as the basic quantity for the localization description of the one-particle state $|\mu\rangle$,

$$S = -\sum_{i=1}^{N} Q_i \ln Q_i . \tag{2.7}$$

This quantity has already been introduced in the characterization of eigenstates [21,30,31]. The single property of S exploited in these studies was that it scales as $\ln N$ for extended states and saturates to a constant for localized states as $N \to \infty$.

As is well known, the Shannon entropy measures the complexity of the distribution $\{Q_i\}$, i.e., the deviation of the actual $\{Q_i\}$ from the uniform distribution $\{Q_i = 1/N, i=1,\ldots,N\}$. The fragmentation of the wave function is a consequence of two physically different internal structures. The primary level of complexity is simply due to the extension of the wave function to D sites of the lattice. Although in the literature D is commonly used as a basic localization quantity, many states with completely different internal structure can result in the same extension D. The simplest of them, carrying the primary level fragmentation, is a steplike function that possesses extension only with no further structure. This state extends over D atoms and has equal ($Q_i = 1/D$) charges on these sites and $Q_i = 0$ on the other $N-D$ ones. Hence the entropy (2.7) of such charge distribution is given as

$$S_{\text{ext}} = \ln D . \tag{2.8}$$

We will define the *extension entropy* for arbitrary states using Eqs. (2.8) and (2.2). The secondary level of complexity of a given state can be identified as a deviation from the steplike functions defined above, which corresponds to the "shape" of the charge distribution $\{Q_i\}$. Therefore the information entropy (2.7) can be given as a sum of two physically different terms [32,33]: the extension entropy S_{ext} (2.8), and the deviation from this value characterizing the shape of the charge distribution, what we may call the *structural entropy*

$$S_{\text{str}} = S - \ln D . \tag{2.9}$$

The well-known properties of the entropy functions

$$0 \le S \le \ln N, \quad 0 \le S_{\text{ext}} \le \ln N \tag{2.10a}$$

are valid; moreover, we have shown that for the structural entropy

$$0 \le S_{\text{str}} \le -\ln q . \tag{2.10b}$$

The detailed proof is given in Appendix A. The last relations will play a basic role in the following considerations.

As S_{ext}, according to Eq. (2.8), is a simple function of D, we may drop S_{ext} as a localization quantity, using instead q as an index for the characterization of the exten-

sion of one-particle states normalized to the size of the system. Furthermore, $S_{\rm str}$ gives an independent description of the localization shape of the wave function. We will show in the next section that the structural entropy restricted by (2.10b) is also normalized properly, in this way making the comparison of localized wave functions in systems of different size possible.

We summarize below some important characteristics of the spatial filling factor q and the structural entropy $S_{\rm str}$ defined by (2.2) and (2.3), and (2.7) and (2.9), respectively.

(i) Both q and $S_{\rm str}$ are independent of any specific order of lattice sites, and any reorganization (permutation) of the distribution $\{Q_i\}$ among lattice sites will lead to identical localization quantities $(q,S_{\rm str})$. This fact shows that the above-defined characterization of localization does not reflect the adjacency relations among atoms of the lattice; it depends only on the distribution of magnitudes of the charges $\{Q_i\}$. In this sense, describing the localization properties of a wave function by the values $(q,S_{\rm str})$ shows the *topology-free* structure of the lattice distribution $\{Q_i\}$.

(ii) Nevertheless, as calculations for real systems show (Sec. VI), the characterization of wave functions by quantities $(q,S_{\rm str})$ gives meaningful results, showing that there exists a topology-free structure in the charge distribution of localized orbitals. This structure is less specific, thus more general, than the usual interpretation of localization. Therefore, we will denote the pair of localization quantities $(q,S_{\rm str})$ as *generalized localization,* which can be easily calculated on fractals, Penrose sets, or for wave functions defined on strange topology lattices, as well.

(iii) The above considerations lead to a very important consequence for charge distributions containing several identical substructures. If the N lattice sites are divided into K identical parts, each consisting of $L=N/K$ sites, the distribution can be written as $\{Q_{k,l}\}=\{\{\tilde{Q}_l,l=1,\ldots,L\},k=1,\ldots,K\}$. Straightforward calculation shows that, using the proper normalization (2.1b) both for $\{Q_{k,l}\}$ and $\{\tilde{Q}_l\}$, the generalized localizations of the total wave function and one of its substructure coincide $(q,S_{\rm str})=(\tilde{q},\tilde{S}_{\rm str})$, i.e., multiplied substructures do not affect the classification scheme of wave functions presented in this paper.

As we will see in numerical applications, most of the information about the localization properties of a given physical system is contained rather in the complete set of the generalized localizations of the eigenstates $\{(q^\mu,S^\mu_{\rm str})\}$ than in one single generalized localization value. The set $\{(q^\mu,S^\mu_{\rm str})\}$, which may be called the *localization map* of the system, can be plotted as a set of points in a *localization diagram* shown in Fig. 1. Restrictions (2.6c) and (2.10b) define an *allowed domain* in the localization diagram, which we have indicated as a shaded area in Fig. 1. This region is universal in the sense that, independently of the system size N, of the dimension of the lattice and of the one-particle function itself, any generalized localization $(q,S_{\rm str})$ must lie in the allowed domain

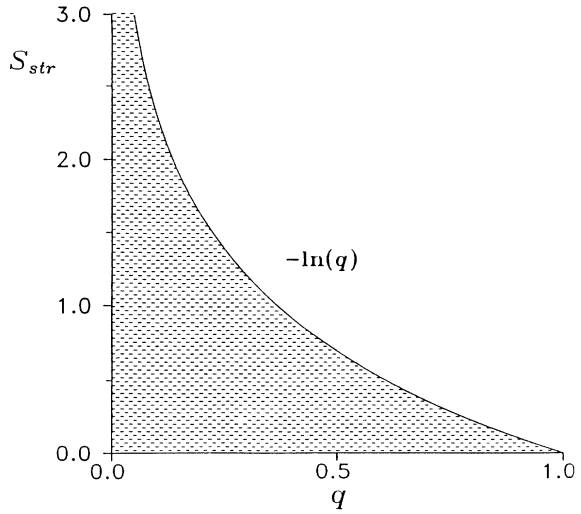

FIG. 1. Allowed domain of the localization diagram. The shaded area represents the region where conditions $0<q\leq 1$ and $0\leq S_{\rm str}\leq -\ln(q)$ are satisfied. The $(q^\mu,S^\mu_{\rm str})$ values of any eigenstate $|\mu\rangle$ should lie in this area.

of the localization diagram. It is possible to prove that the opposite statement is also true (see Appendix B): the allowed domain is the most confined area in the localization diagram, i.e., to any given preselected point $(\bar{q},\bar{S}_{\rm str})$ from the allowed domain there exists a system size N and a wave function such that the corresponding generalized localization $(q,S_{\rm str})$ value is arbitrarily close to $(\bar{q},\bar{S}_{\rm str})$.

On the other hand, we will see below that different localization shapes specify characteristic regions in the allowed domain, in this way making the distinction of various localization forms possible.

III. THE CONTINUOUS LATTICE MODEL

"Localization" in the classical interpretation means the ascending behavior of the wave function according to a given shape as the function of distance r measured from the "center" of the wave function. This description, however, contains the ill-defined concept of "center" of one-particle states and it is hardly applicable to fractal lattices and highly random systems where closeness and neighborhood relations lose their original meaning. Moreover, numerical calculations have shown that wave functions in disordered systems are very often multipeaked and noisy, which does not fit in the classical picture (see, e.g., Sec. VI B).

We recall here, however, the property of the generalized localization $(q,S_{\rm str})$ mentioned in the previous section. If the wave function is composed of some peaks with similar internal structure, the $(q,S_{\rm str})$ values calculated for the total wave function will be essentially the same as for a single peak alone. On the other hand, as both q and $S_{\rm str}$ are obtained by summation for all lattice sites, they can be considered as "integral" quantities, which causes the noisy behavior of the orbitals to be eliminated in calculating $(q,S_{\rm str})$.

Thus the overall localization shape of the peaks of a

complicated noisy wave function can be represented by a one-peak spherically symmetric smooth decay function, as far as the $(q,S_{\rm str})$ values are concerned. We will show in this section that a given wave-function shape defines a strict functional relation between the generalized localization quantities $(q,S_{\rm str})$. Studying this relation for a given system, conclusions for the localization shape of the wave functions can be drawn. The one-peak representation of the wave functions covers even a broader class; e.g., surface states, which are essentially half-peak shaped. A full peak, in fact, can be divided into two identical half-peaks, so the above argumentation remains in effect in this case as well.

A. Notations, definitions

In order to find an analytic relation between the overall localization shape and the generalized localization we introduce the *continuous lattice model* (CLM) assuming that all characteristic distances (i.e., the localization length of a given one-electron function and the linear size of the system) are large compared to the interatomic distances. We also assume that the charge distribution of the localized orbital to be studied can be made equivalent in the above way, with a spherically decaying form function f, and we place the origin of the system of reference to its maximum position. The charge of this reference distribution on site i is described by the ansatz

$$Q_i=Q(r_i)=Af(r_i/\lambda)\ , \tag{3.1}$$

where r_i is the distance of site i measured from the maximum position of the charge distribution, A is the maximum amplitude, and λ is the localization length. Function $f(\rho)$ describes the shape of the envelope of the charge distribution and it will play a central role in the following considerations. The envelope function $f(\rho)$ referred to later on as the decay form function (DFF) obeys the following relations:

$$f(0)=1\ , \tag{3.2a}$$

$$0\le f(\rho)\le 1 \quad \text{for } 0\le\rho<\infty\ . \tag{3.2b}$$

The asymptotic long-distance behavior of $f(\rho)$ $(\rho\to\infty)$ can be different for various decay forms; this property will be used in Sec. V to classify different localization classes.

Within the CLM approach we consider the distribution (3.1) being embedded in a large but finite atomic system of radius R, and assume that the atomic network can be replaced by a homogeneous medium with uniform atomic density n. (For perfect crystals $n=m/\omega$, where ω is the volume of the unit cell and m is the number of atoms in it.) In this way we replace all lattice sums by integrals of the form

$$\sum_i(\cdots)_i\to\int_0^R(\cdots)n_d(r)dr\ , \tag{3.3a}$$

where

$$n_d(r)=ns_dr^{d-1} \tag{3.3b}$$

is the spherical density of lattice sites, d is the Hausdorff dimension of the atomic network that can be noninteger for fractals, and s_d is the surface of the mathematical d-dimensional unit sphere (e.g., $s_1=1$, $s_2=2\pi$, $s_3=4\pi$).

B. General formulation

Now we transform four important lattice sums into integrals in the following way:

$$N=\sum_{i=1}^{N}1\to N=\int_0^R n_d(r)dr=ns_d\frac{R^d}{d}\ , \tag{3.4a}$$

$$1=\sum_{i=1}^{N}Q_i\to 1=\int_0^R Af(r/\lambda)n_d(r)dr\ , \tag{3.4b}$$

$$D^{-1}=\sum_{i=1}^{N}(Q_i)^2\to D^{-1}=\int_0^R A^2f^2(r/\lambda)n_d(r)dr\ , \tag{3.4c}$$

$$S=-\sum_{i=1}^{N}Q_i\ln Q_i$$

$$\to S=-\int_0^R Af(r/\lambda)\ln[Af(r/\lambda)]n_d(r)dr\ . \tag{3.4d}$$

Let us introduce the following functionals:

$$E\{f,d,z\}\equiv E(z)=\int_0^z\rho^{d-1}d\rho=\frac{z^d}{d}\ , \tag{3.5a}$$

$$F\{f,d,z\}\equiv F(z)=\int_0^z f(\rho)\rho^{d-1}d\rho\ , \tag{3.5b}$$

$$G\{f,d,z\}\equiv G(z)=\int_0^z f^2(\rho)\rho^{d-1}d\rho\ , \tag{3.5c}$$

$$H\{f,d,z\}\equiv H(z)=-\int_0^z f(\rho)\ln f(\rho)\rho^{d-1}d\rho\ , \tag{3.5d}$$

where for a given DFF f and dimension d we use the shorthand notations $E(z)$, $F(z)$, $G(z)$, and $H(z)$. Using the above definitions, Eq. (3.3b), and the substitution $\rho=r/\lambda$, we obtain from (3.4)

$$N=ns_d\lambda^dE(z)\ , \tag{3.6a}$$

$$1=Ans_d\lambda^dF(z)\ , \tag{3.6b}$$

$$D^{-1}=A^2ns_d\lambda^dG(z)\ , \tag{3.6c}$$

$$S=Ans_d\lambda^d[H(z)-\ln(A)F(z)]\ , \tag{3.6d}$$

where $z=R/\lambda$. Dividing Eqs. (3.6a), (3.6c), and (3.6d) by Eq. (3.6b) and using definitions (2.3), (2.7), and (2.9), we arrive at the generalized localizations within the CLM approach

$$q(z)=\frac{F^2(z)}{E(z)G(z)}\ , \tag{3.7a}$$

$$S_{\rm str}(z)=\frac{H(z)}{F(z)}+\ln\frac{G(z)}{F(z)}\ . \tag{3.7b}$$

It is clear from Eqs. (3.7) that both q and $S_{\rm str}$ are expressed in a parametric form depending only on the DFF and the dimension d of the system.

It is also possible to show that for any $0\le z<\infty$ the generalized localization $(q(z),S_{\rm str}(z))$ of the CLM lies, similarly to the discrete case, in the allowed domain of the localization diagram defined in Sec. II,

$$0<q(z)\le 1\ , \tag{3.8a}$$

$$0\le S_{\rm str}(z)\le -\ln q(z)\ . \tag{3.8b}$$

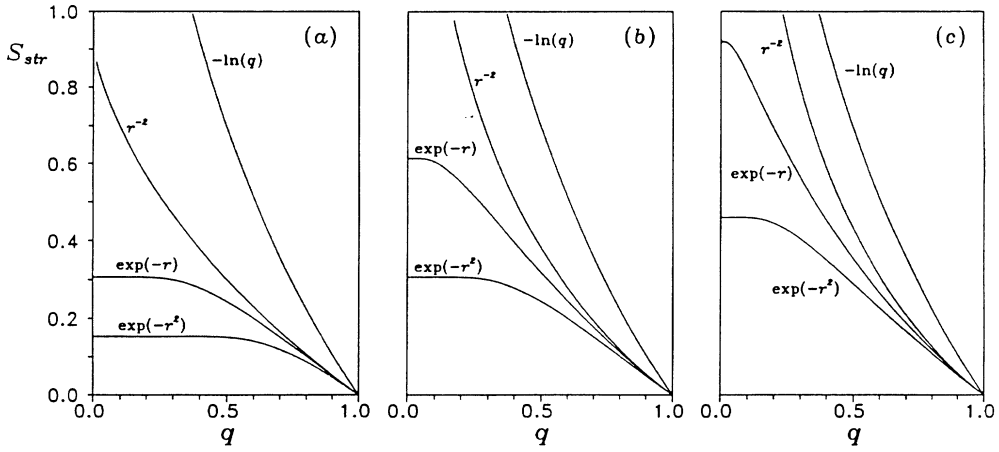

FIG. 2. Structural entropy $S_{\rm str}$ vs filling factor q reference curves for decay form functions with Gaussian $f(r)=\exp(-r^2)$, exponential $f(r)=\exp(-r)$, and power-law $f(r)=(1+r)^{-2}$ decay. The curves are labeled by the asymptotic behavior of the corresponding decay form function. The limiting curve of the allowed domain $-\ln(q)$ is also indicated. The parts of the figure show the universal reference curves for dimensions (a) $d=1$, (b) $d=2$, (c) $d=3$.

The detailed proof can be found in Appendix A.

The set $\{(q(z),S_{\rm str}(z));\ 0\le z<\infty\}$ for a given envelope function f and dimension d corresponds to a unique curve in the allowed domain of the localization diagram. The curve is independent of the system size R (i.e., the number of lattice sites N), the amplitude A of the charge distribution, the localization length λ, and the topology of the lattice and of the atomic density. Explicit formulas are elaborated in Appendix C for these universal reference CLM curves in the cases of exponential $f(\rho)=\exp(-\rho)$, Gaussian $f(\rho)=\exp(-\rho^2)$, and power-law DFF's $f(\rho)=(1+\rho)^{-m}$ in various dimensionalities. Figure 2 shows that the calculated lines are well separated in the allowed domain. This property and the universality of the CLM curves make the detection of various localization shapes in real systems possible. The basic classification idea is plotting the localization map of the studied system and comparing it with the reference CLM lines, which gives information about the localization shape of the one-electron eigenfunctions. Since universal CLM curves serve as reference lines, adequate precision polynomial fits are also given in Appendix C in order to ease further usage.

C. Limit of the CLM approximation

The CLM is expected to break down if the localization length λ becomes comparable to the interatomic distance a ($\lambda\sim a$); therefore the extension of the orbital $D\sim 1$, or according to Eq. (2.3),

$$q\sim\frac{1}{N}\ . \tag{3.9}$$

The applicability of the CLM according to (3.9) is defined by a minimum localization length λ_0, requiring the following relationship:

$$q\left[\frac{R}{\lambda_0}\right]=\frac{1}{N}\ , \tag{3.10}$$

where function $q(z)$ is given by Eq. (3.7a).

In order to estimate the magnitude of λ_0 let us consider a simple d-dimensional cubic lattice with atomic density $n=a^{-d}$. In this case Eq. (3.4a) becomes

$$N=\frac{S_d}{d}\left[\frac{R}{a}\right]^d\ . \tag{3.11}$$

Assuming exponential-type localization with large $z_0=R/\lambda_0$, we can apply the asymptotic form of Eq. (C2)

$$q(z)\approx d2^{-d}\Gamma(d)z^{-d}\ , \tag{3.12}$$

where $\Gamma(d)$ is the complete gamma function. Introducing Eqs. (3.11) and (3.12) into condition (3.10), we arrive at

$$\frac{\lambda_0}{a}=\tfrac{1}{2}[s_d\Gamma(d)]^{-1/d}=\begin{cases}0.50 & \text{if } d=1,\\ 0.20 & \text{if } d=2,\\ 0.17 & \text{if } d=3\ .\end{cases} \tag{3.13}$$

For a Gaussian decay we obtain similarly

$$\frac{\lambda_0}{a}=\begin{cases}0.80 & \text{if } d=1,\\ 0.40 & \text{if } d=2,\\ 0.40 & \text{if } d=3\ .\end{cases} \tag{3.14}$$

Since λ_0 in all of the above cases (and especially in higher dimensions) is small compared to the lattice constant, and validity of the CLM is expected to cover a broad range of localization length values.

IV. EXTREME DELOCALIZATION

We wish to discuss here some further properties of the $q\mapsto S_{\rm str}$ relation for extremely delocalized wave functions. In the discrete lattice model this situation is characterized by an arbitrary small perturbation of the uniform charge distribution

$$Q_i = 1/N + \delta_i \ , \tag{4.1a}$$

where

$$|\delta_i| \ll 1/N \ . \tag{4.1b}$$

Normalization (2.1b) requires

$$\sum_{i=1}^{N} \delta_i = 0 \ . \tag{4.2}$$

Keeping first- and second-order terms of δ_i only, one easily gets from definitions (2.2), (2.3), (2.7), and (2.9),

$$q \approx 1 - N \sum_{i=1}^{N} \delta_i^2 \ , \tag{4.3a}$$

$$S_{\text{str}} \approx \frac{N}{2} \sum_{i=1}^{N} \delta_i^2 \ . \tag{4.3b}$$

This result shows that for the completely delocalized charge distribution $q=1$, $S_{\text{str}}=0$, while for arbitrary wave functions close to it, the structural entropy behaves approximately as

$$S_{\text{str}} \approx \frac{1-q}{2} \ . \tag{4.4}$$

In the continuous lattice model an extremely delocalized state of arbitrary shape arises if the localization length λ becomes large compared to the system size R. This corresponds to the limit $z = R/\lambda \to 0$. We have shown in Appendix D that for extreme delocalization

$$\lim_{z\to 0} q(z) = 1, \quad \lim_{z\to 0} S_{\text{str}}(z) = 0 \ . \tag{4.5}$$

It is also possible to detect the universal behavior around the $q=1$ point. The slope of the $q \mapsto S_{\text{str}}$ curve at the completely delocalized point $z=0$, $q=1$, $S_{\text{str}}=0$ is

$$\alpha = \lim_{q\to 1} \frac{dS_{\text{str}}}{dq} = \lim_{z\to 0} \frac{S'_{\text{str}}}{q'} = -\frac{1}{2} \ , \tag{4.6}$$

where the prime means the first derivative with respect to variable z. The proof is given in Appendix D.

The above facts indicate that the behavior of the CLM curves in the completely delocalized region is identical for all decay forms, and approximation (4.4) of the discrete model holds here as well. The physical interpretation of this result is that it is impossible to identify decay forms for almost completely delocalized wave functions.

V. THREE CLASSES OF LOCALIZATION

We will study now the behavior of various decay shapes in the extremely localized limit when the localization length λ becomes negligible compared to the system size R. Mathematically this case corresponds to $z = R/\lambda \to \infty$. Although this happens if R is constant and $\lambda \to 0$, the situation is out of the scope of the CLM, since the basic assumptions of the model described in Sec. III are not satisfied in this case. On the other hand, if the localization length λ remains constant, but the radius R of the system grows to infinity, the question of extreme localization keeps its relevance even in the continuous lattice model.

According to the general behavior of the envelope form function $f(z)$ at least three different classes of localized wave functions can be distinguished. Defining $f(z)$ in Sec. III we insisted by conditions (3.2) that the DFF should not "explode" in any direction. This restriction, however, includes strictly delocalized functions as well, since

$$\lim_{z\to\infty} f(z) = 1 \tag{5.1}$$

is characteristic for complex Bloch functions, while those functions for which (3.2b) holds but limit (5.1) does not exist are typically oscillatory wave functions, like real Bloch waves.

The first broad class of localized functions will be defined as a set of decay form functions, which are not strictly delocalized, i.e.,

$$\lim_{z\to\infty} f(z) = 0 \ . \tag{5.2}$$

This set can be called *decay localized* and will be denoted by L_d.

A more restrictive definition of localization requires that the wave function should not fill out the complete lattice as the size of the system increases. This condition leads to the class of *filling localized* functions L_f, for which

$$\lim_{z\to\infty} q(z) = 0 \ . \tag{5.3}$$

Since the filling factor has been defined in (2.3) as the relative extension of the wave function compared to the system size, L_f does not contain finite-sized functions only. For increasing system radius R, wave functions with continuously growing extension D can be still *filling localized* if D tends to infinity slower than the number of atoms N itself.

On the other hand, the class of finite-sized functions L_s is defined by the relation

$$\lim_{z\to\infty} D(z) < \infty \ . \tag{5.4}$$

For finite systems we always suppose the normalization of the one-electron functions. We can consider the set of decay functions *norm localized,* where the possibility of normalization is still kept with arbitrarily increasing system size R (i.e., they remain normalizable in limit),

$$\lim_{z\to\infty} F(z) < \infty \ . \tag{5.5}$$

The class of *norm localized* functions will be denoted by L_n.

The various relations among different localization definitions are discussed in Appendix E. We have shown there that for "nonexploding" envelopes (3.2) the classes of finite-sized and *norm localized* wave functions are equivalent

$$L_s \equiv L_n \ . \tag{5.6}$$

On the other hand, classes L_d, L_f, and L_n are essentially

different and the following strict containment relations hold:

$$L_d \supset L_f \supset L_n \ . \tag{5.7}$$

This result shows that *norm localized* functions are *filling localized* and all *filling localized* functions are *decay localized* at the same time. In contrast, there exist envelope form functions (e.g., with power-law decay) that decay to zero, but they always fill out a commensurate part of any lattice and they are not normalizable as well. An interesting result is that there exist wave functions that occupy a negligible part of the whole lattice only *(filling localized)* but they are still not normalizable in infinite lattices.

VI. APPLICATIONS

In this section we present some examples showing the wide range of applicability of the method described in the previous sections. We have included the problem of noisy charge distributions, the properties of wave functions near the metal-insulator transition in one-dimensional quasiperiodic systems, some unusual behavior of self-consistent-field (SCF) eigenstates of aromatic hydrocarbons, and finally the role of dynamical disorder in two-dimensional disordered tight-binding systems.

A. White-noise distribution

Since the charge distribution of one-electron eigenfunctions obtained in actual calculations for molecules or disordered systems frequently appears to be quite irregular at first sight, we will study here a completely random distribution without any specific structure, in order to be able to extract information from noisy one-electron wave functions. For simulating this case we have chosen a completely delocalized charge distribution superimposed by a white-noise perturbation on each site with weight w,

$$Q_i = \frac{1+w\xi_i}{\sum_{j=1}^{N}(1+w\xi_j)} \ . \tag{6.1}$$

The weight factor w varies between 0 and ∞ and ξ_i are independent random variables of uniform distribution over the [0,1) interval. With $w=0$ we arrive at a completely delocalized wave function, while $w\to\infty$ gives a white-noise charge distribution.

Besides Monte Carlo simulations, it is possible to get analytical results for arbitrary w in the case of large lattices. We will utilize the fact that according to the central-limit theorem for large enough N,

$$\sum_{j=1}^{N}(1+w\xi_j) \approx N\langle 1+w\xi_j\rangle = N(1+w/2) \ , \tag{6.2}$$

where the expectation value of any function η of the random variable ξ is defined as

$$\langle \eta \rangle = \int_0^1 \eta(\xi)d\xi \ . \tag{6.3}$$

It is easy to show that $\langle \xi_i \rangle = \frac{1}{2}$, $\langle \xi_i^2 \rangle = \frac{1}{3}$, and since variables ξ_i and ξ_j are independent on different sites, $\langle \xi_i \xi_j \rangle = \langle \xi_i \rangle \langle \xi_j \rangle$ if $i \neq j$.

Applying approximation (6.2), the calculation of the expectation value of (2.2) is straightforward, resulting in the filling factor

$$\langle q \rangle = \frac{3}{4}\frac{(2+w)^2}{3+3w+w^2} + \frac{1}{4N}\frac{w^2}{3+3w+w^2} \ . \tag{6.4}$$

As the second term is bounded for $w\in[0,\infty)$ it can be neglected for large N (the relative error is in fact less than 0.1 if $N>3$), which gives

$$\langle q \rangle = \frac{3}{4}\frac{(2+w)^2}{3+3w+w^2} \ . \tag{6.5}$$

For the structural entropy we get

$$\langle S_{\rm str} \rangle = \langle S \rangle - \langle \ln D \rangle \approx \langle S \rangle - \ln\langle D \rangle = \langle S \rangle - \ln\langle q \rangle - \ln N \ . \tag{6.6}$$

The approximation used above is based on the fact that D is a large argument of the slowly varying logarithm function, as according to (6.5) $\frac{3}{4} \le \langle q \rangle \le 1$ and $\langle D \rangle \propto N$. The detailed calculation using (2.7) and (6.2) yields

$$\langle S_{\rm str} \rangle = \frac{1}{2} - \ln\frac{3}{2} + \ln\frac{2+w}{1+w} - \frac{\ln(1+w)}{w(2+w)} - \ln\frac{(2+w)^2}{3+3w+w^2} \ . \tag{6.7}$$

Expressions (6.5) and (6.7) for $w\to 0$ satisfy the general properties obtained for completely delocalized wave functions previously and, on the other hand, any random distribution (6.1) is more delocalized than the ideal white-noise wave function ($w\to\infty$)

$$\tfrac{3}{4} = \lim_{w\to\infty}\langle q \rangle \le \langle q \rangle \le \lim_{w\to 0}\langle q \rangle = 1 \ , \tag{6.8a}$$

$$\tfrac{1}{2} - \ln(\tfrac{3}{2}) = \lim_{w\to\infty}\langle S_{\rm str} \rangle \ge \langle S_{\rm str} \rangle \ge \lim_{w\to 0}\langle S_{\rm str} \rangle = 0 \ . \tag{6.8b}$$

In order to check the validity of the various approximations used in the derivation of formulas (6.5) and (6.7) we have carried out numerical Monte Carlo calculations for random charge distributions (6.1) on a lattice with $N=10\,000$ sites. The results show excellent agreement with the continuous curve corresponding to the parametric representation (6.5) and (6.7) of the $(q, S_{\rm str})$ relation. As is seen in Fig. 3, these kinds of "noisy" orbitals are considered rather delocalized. The localization behavior is independent of the dimension d of the lattice and imitates a one-dimensional (1D) Gaussian decay. Although the $(\langle q \rangle, \langle S_{\rm str} \rangle)$ curve definitely differs from the one with the exact 1D Gaussian decay, it is still expected that due to statistical fluctuations the localization map resulting from actual calculations of delocalized 1D Gaussian wave functions will be indistinguishable from a white-noise distribution. A similar result was found for the eigenfunctions of random matrices where the individual vector components asymptotically follow a Gaussian distribution in the $N\to\infty$ case [34].

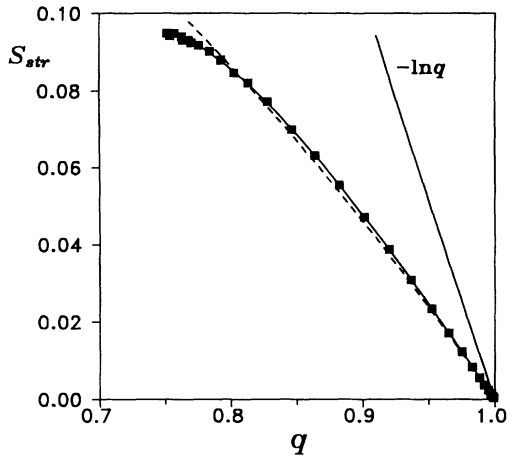

FIG. 3. Structural entropy $S_{\rm str}$ vs filling factor q for white-noise distribution. The solid line stands for analytic results [see Eqs. (6.5) and (6.7)] and solid squares show the results of numerical simulations. They are compared to the curve for one-dimensional Gaussian decay (dashed curve). The curve for $-\ln q$ is also indicated.

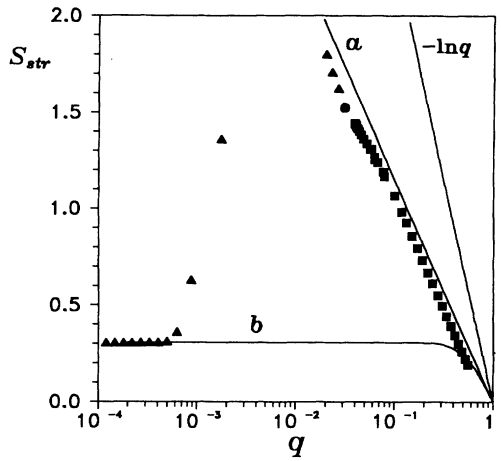

FIG. 4. Structural entropy $S_{\rm str}$ vs filling factor q of states around E_c on a linear-logarithmic scale. Curve labeled a is for power-law decay $(1+r)^{-1}$ in one dimension, b for exponential decay. The curve for $-\ln q$ is also indicated. Solid symbols represent the results of numerical calculation $\lambda=1.0$ ($E_c=1.0$), $\alpha=4.0$, $\nu=0.1$, and $N=10^5$. Squares and triangles correspond to states with $E<E_c$ and $E>E_c$, respectively, while a solid circle stands for the state at the mobility edge $E=E_c$. The energy range of the states plotted is $0.9<E<1.1$.

B. One-dimensional quasiperiodic system

One-dimensional systems with incommensurate potential have proved to be good models for the numerical investigation of the delocalization-localization transition, i.e., the metal-insulator transition [35]. In this case the discretized one-dimensional tight-binding Schrödinger equation within the nearest-neighbor approximation is written in the recursive form

$$u_{n+1}+u_{n-1}-(V_n-E)u_n=0\ , \tag{6.9}$$

where u_n is the amplitude of the eigenstate on the nth lattice site, V_n is the on-site (diagonal) quasiperiodic potential, and E is the eigenenergy. The nearest-neighbor transfer integral is assumed to be the unit of the energy scale.

In our study, based on the work of Das Sharma, He, and Xie [36], we have chosen a slowly varying potential of the form

$$V_n=\lambda\cos(\pi\alpha n^{\nu})\ , \tag{6.10}$$

which produces a gapless spectrum containing mobility edges at the critical energy $E_c=\pm|2-\lambda|$ if $0<\nu<1$, implying a metal-insulator transition at $\lambda_c=2-|E|$ for a given energy E. We have investigated the localization properties of the states in the vicinity of the mobility edge.

In Fig. 4 we have plotted the $S_{\rm str}$ versus q values for the eigenstates in the vicinity of the mobility edge for $\lambda=1$, $E_c=1$ using $\nu=0.1$, and $\alpha=4.0$, and systems of the size $N=10^5$. The states marked with solid squares and triangles are the ones with $E<E_c$ and $E>E_c$, respectively. The solid circle indicates the state at $E=E_c$. The states towards the band center ($E<E_c$) are clearly on the curve that is characteristic of a power-law decay $f(\rho)=(1+\rho)^{-1}$, while most of the states towards the band edge seem to be exponentially localized. Running λ for a fixed energy E around the metal-insulator transition gives a very similar picture [37].

As further evidence of this conclusion we have plotted the charge distribution, i.e., the square modulus of the coefficients ($Q_n=|u_n|^2$) of the wave function (without normalization) at the mobility edge in Fig. 5. For comparison, the shape of the potential [cf. Eq. (6.10)] is also shown. One can clearly see that there are significant peaks at the position of the minima of the potential. A detailed analysis of this result is published elsewhere [37].

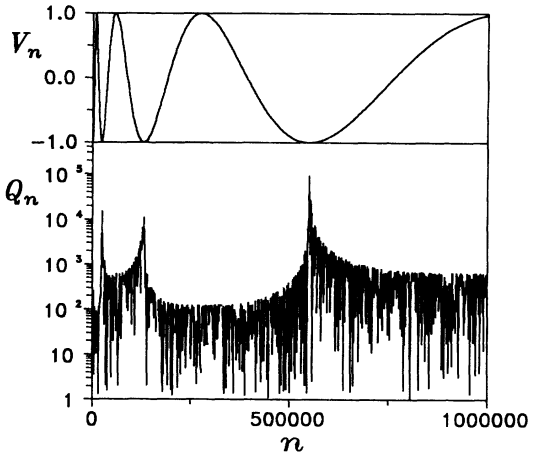

FIG. 5. Quasiperiodic potential V_n and the resultant charge distribution Q_n of the wave function at the mobility edge over a chain of length $N=10^6$. The parameters are $\lambda=1.0$, $E=1.0$, $\alpha=4.0$, and $\nu=0.1$. The wave function has not been normalized. Note that the peaks in Q_n are at the same place as the minima in the potential V_n.

We have to emphasize that, in spite of the multipeaked structure of the wave function, the localization diagram clearly shows a power-law behavior.

C. Planar molecules

Delocalized π-electron systems of planar alternating and aromatic hydrocarbon molecules are expected to be excellent targets for modeling metallic conduction in one and two dimensions. The finite size of molecules, on the other hand, may lead to the appearance of surface states, as well as charge fluctuations on the skeleton carbon atoms. It has been shown [38], however, that charge inhomogeneities imply electron localization.

For tracing charge rearrangements an iterative solution of the one-particle effective Schrödinger equation is necessary. The most simple SCF Hartree-Fock description of π-electron systems can be accomplished by using the so-called Pariser-Parr-Pople (PPP) method [39], which separates π electrons from the σ-bond skeleton of the molecules. The PPP Hamiltonian reads as

$$H_{ij}=\begin{cases} U_i+\frac{1}{2}P_{ii}\gamma_{ii}+\sum\limits_{k\ (\neq i)}(P_{kk}-Z_k)\gamma_{ik} & \text{if } i=j, \\ \beta_{ij}-\frac{1}{2}P_{ij}\gamma_{ij} & \text{if } i\neq j\ . \end{cases} \tag{6.11}$$

The i and j site indices run over the carbon atoms of the molecules, U_i are atomic parameters, and Z_i denotes the screened nuclear charge of atom i. The values of β_{ij} are parameters of the theory and describe the bond strength between atoms i and j. The effective electron-electron interaction part of the Hamiltonian corresponds to those terms in (6.11) that contain the one-electron density matrix elements

$$P_{ij}=2\sum_{\mu} c_i^{\mu}c_j^{\mu}\ . \tag{6.12}$$

The summation runs over the occupied one-electron orbitals $|\mu\rangle$, with expansion coefficient c_i^{μ} on site i. A spin factor of 2 is applied for accounting for double occupancy. The Coulomb interaction of two electrons placed on sites i and j is γ_{ij}, which are approximated by the Mataga-Nishimoto formula

$$\gamma_{ij}=\frac{e^2}{R_{ij}+a_{ij}} \quad \text{with } a_{ij}=\frac{2e^2}{(\gamma_{ii}+\gamma_{jj})}\ , \tag{6.13}$$

where e is the electron charge and R_{ij} is the distance between the sites i and j. In the usual parametrization of the method for carbon atoms $U_i=-11.22$ eV, $\gamma_{ii}=-10.53$ eV, $\beta_{ij}=-2.4$ eV for nearest neighbors, and $\beta_{ij}=0$ otherwise [40].

The eigenvalue problem of the Hamiltonian (6.11) is solved iteratively by the SCF technique. The PPP procedure is closely related to the Hückel or tight-binding method, which is widely used in solid-state physics for electron-structure calculations.

We have carried out calculations for a series of alternating and aromatic hydrocarbon molecules and analyzed the localization characteristics of the wave function. A detailed study is published elsewhere [32], and we will discuss here only some typical aspects of the results by comparing two similar molecules, chrysene and benz[a]anthracene, which are shown in Fig. 6. Each of the molecular graphs can be transformed into the other by the transposition of one hexagonal cell of the network. The localization map $\{(q^{\mu},S_{\rm str}^{\mu})\}$ for all (occupied and virtual) PPP eigenfunctions $|\mu\rangle$ of both molecules is plotted in Fig. 7. As a consequence of the well-known pairing theorem for alternate hydrocarbons the structural entropy and filling factor of the related occupied and virtual orbital pairs coincide.

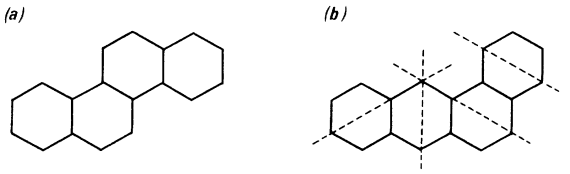

FIG. 6. Molecular graphs of (a) chrysene and (b) benz[a]anthracene. Only the carbon skeleton is shown. In the case of benz[a]anthracene, dashed lines indicate the position of nodal surfaces in the CDW state.

As is seen, the wave functions are far from being completely delocalized, but still can be considered moderately extended ($0.5<q<0.8$). The shape characteristics of the orbitals are in the intermediate range between 1D Gaussian and 1D exponential (or 2D Gaussian). The only remarkable difference found between the two molecules is the appearance of an eigenstate with a low $S_{\rm str}$ value at $q\approx 0.55$ in benz[a]anthracene. $S_{\rm str}\approx 0$ indicates a steplike behavior of the wave function, and a further analysis of the coefficients c_i shows that this curious orbital has nodal surfaces along the dashed lines in Fig. 6(b), whereas

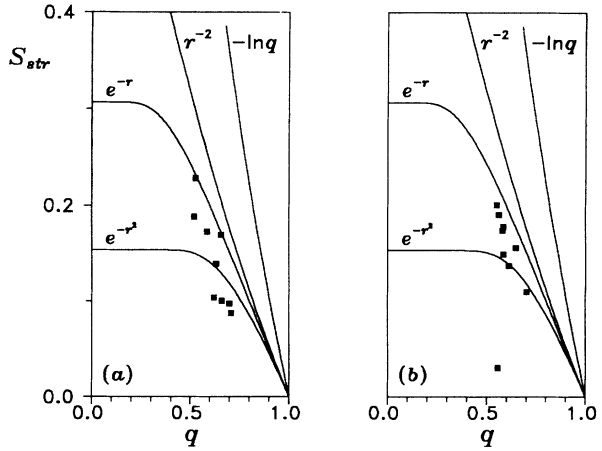

FIG. 7. Localization maps of (a) chrysene and (b) benz[a]anthracene. The reference CLM curves are labeled by the asymptotic behavior of the corresponding decay form function. The limiting curve of the allowed domain $-\ln q$ is also indicated. In the chrysene no CDW states can be identified, while in the localization map of benz[a]anthracene a state close to the horizontal axis appears indicating CDW-like behavior. The schematic illustration of the corresponding wave function is shown in Fig. 6(b).

the charges of other atoms are almost equal. Similar wave functions were found and identified as bond-centered charge-density waves (CDW's) in SCF studies on one-dimensional metals [41]. Our result shows that bond-centered CDW's also appear in two-dimensional molecules, but the existence of these states seems to be strongly dependent on the topological structure of the system. As the detailed study on a larger set of molecules [32] has proved, the above conclusions generally hold for all aromatic hydrocarbon systems under consideration.

D. Localization in 2D

The phenomenon of localization is not fully understood in two-dimensional systems. There is still a vivid interest concerning this problem (see, e.g., Ref. [42]); therefore we have also investigated the localization problem of off-diagonal disorder using a tight-binding model over a two-dimensional $n \times n$ lattice with periodic boundary conditions. It was essentially described by the Hamiltonian [43]

$$H=\sum_i |i\rangle \varepsilon_0 \langle i| + \sum_{i,j} |i\rangle V_{ij} \langle j| \ , \tag{6.14}$$

where $|i\rangle$ and $|j\rangle$ denote one-electron orbitals centered on sites i and j, and ε_0 is the site excitation energy. $V_{ij}=V(r_{ij})$ is the transfer integral chosen in the modified exponential form

$$V(r)=-V_0(1+r/a)\exp(-r/a) \ , \tag{6.15}$$

where r_{ij} is the distance between sites i and j, and a is the effective interaction length. The parameter V_0 is set so that $V_1=V(r_{ij}=a)=-1$ is obtained. The transfer integral is assumed to have a finite cutoff range r_c. Hence the second summation in Eq. (6.14) runs over all sites $i \neq j$ and $0<r_{ij} \leq r_c$. Therefore the number of neighbors Z_i of a given site i can be defined as the number of sites within the cutoff range.

The underlying structure is a regular square lattice with random distortions. Periodic boundary conditions are imposed. Starting from a 2D square lattice with lattice constant a, each site was shifted to the arch of a circle of its original position as the imitation of its thermal motion. We have chosen the same radius δr for all sites and random angle θ with uniform distribution over the interval $0<\theta \leq 2\pi$ with respect to the x axis. Therefore the parameter describing the strength of disorder is [43]

$$\eta=\delta r/a \ . \tag{6.16}$$

Beyond the off-diagonal disorder arising from the distortions described above, dynamical disorder enters in the Hamiltonian (6.14) by letting the cutoff range depend on η, which is an indication of the coupling between electrons and lattice vibrations. In the simplest approximation we may set [44]

$$r_c=a(1+2\eta) \ , \tag{6.17}$$

with the allowed range being $0 \leq \eta \leq 0.5$. Under such conditions the off-diagonal parameters V_{ij} in the Hamiltonian will have a uniform distribution in the range [44] $V_1(1-\eta)<V_{ij}<V_1(1+\eta)$. Note that the same parameter η appears for both the description of disorder in the Hamiltonian as well as that of the lattice. As a consequence, this model yields a simulation of the electron-phonon coupling or the behavior of electrons moving in the stochastic medium studied in Ref. [45], and resembles some features of the model introduced recently by Dunlap and co-workers [23].

Using the Hamiltonian in Eq. (6.14), we have calculated the eigenstates of several samples by means of direct diagonalization. It was already shown [44] that for small $0<\eta<\eta_c$ the states remain extended, while for $\eta>\eta_c$ weakly localized states appear. The critical parameter η_c is the amount of disorder at which those sites, which were second nearest neighbors in the absence of disorder, start to have a nonzero transfer integral. Its value depends on the lattice geometry; in our case $\eta_c=(\sqrt{2}-1)/4$.

In Fig. 8 we have plotted a cumulative picture of the states of a few samples of 20×20 lattices for $\eta=0.3$. One can clearly observe a strong correlation of the $S_{\rm str}$ and q values, which is due to the complex nature of the spatial behavior of the wave functions. The observed $S_{\rm str}(q)$ relation can be fairly well reproduced; for instance, by a decay form function with a short-range exponential and a Friedel-oscillation tail

$$f(\rho)=\begin{cases} \exp(-\rho) & \text{if } \rho \leq R_0, \\ A\dfrac{\cos(\alpha\rho+\varphi)+1}{\rho^2} & \text{if } \rho \geq R_0 \ . \end{cases} \tag{6.18}$$

with $\alpha=10$ and $R_0=0.75$. Parameters A and φ are determined according to the requirement that $f(\rho)$ and

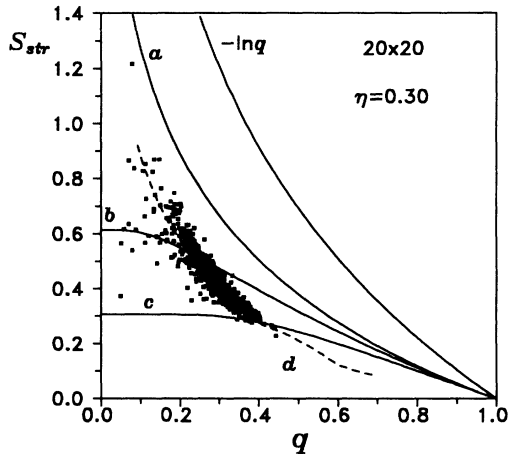

FIG. 8. Structural entropy $S_{\rm str}$ vs filling factor q for the model of off-diagonal disorder. The curve labeled a is for quadratic decay $(1+r)^{-2}$ in two dimensions, curve b is for exponential, and curve c is for Gaussian decay. Solid squares represent our calculation of the eigenstates of a few samples of 20×20 lattices with periodic boundary conditions. The disorder parameter $\eta=0.3$. The dashed curve stands for modeling Friedel-oscillation-like behavior [see Eq. (6.18)].

$df(\rho)/d\rho$ should be continuous at $\rho=R_0$. The dashed line in Fig. 8 corresponds to (6.18).

VII. SUMMARY

In this paper we have introduced a classification scheme for the characterization of one-particle states in real space. Our method consists of the simple calculation of two localization indices, the filling factor q that is derived from the participation ratio and a localization parameter, the structural entropy $S_{\rm str}$. Although q and the Shannon entropy S have been used separately by several authors, we have shown that there exists a universal relation between q and $S_{\rm str}$ that depends only on the decay form of the wave function and the dimension d of the underlying atomic network. This relation behaves uniformly in the extreme delocalization limit, as it should, and shows variations at the extreme localization limit. The $S_{\rm str}(q)$ function may be calculated for ideal decay form functions, which we have given for the case of Gaussian, exponential, and power-law decays in dimensions $d=1,2,3$. The implementation of our method in already existing program systems is particularly easy, based on Eqs. (2.2) and (2.3), and Eqs. (2.7) and (2.9), together with the explicit reference curves given in Appendix C. We would like to mention that this kind of shape analysis is independent of other methods used for the description of the wave functions (e.g., multifractal analysis [17,20]). In actual numerical calculations, the localization map of the system, which is the set $\{(q^{\mu},S^{\mu}_{\rm str})$ for all eigenfunctions $|\mu\rangle\}$, is compared to the ideal CLM curves. This leads to useful physical conclusions.

ACKNOWLEDGMENT

This work was supported by the Országos Tudományos Kutatási Alap (OTKA), Grant Nos. 406 and 517/1991.

APPENDIX A: THE ALLOWED DOMAIN OF THE LOCALIZATION DIAGRAM

The proof of some basic relations for the structural entropy $S_{\rm str}$ given in (2.10) for discrete charge distributions and in (3.8) in the continuous lattice limit follows from the well-known *Jensen's inequality* of analysis. Although it can be formulated in a general way using the *Lesbegue integration* technique, we will cite here only two particular cases.

Theorem 1: Discrete form of Jensen's inequality. If function $\mathcal{L}$: $\mathbb{R}\to\mathbb{R}$ is convex and continuous on the interval (a,b), then for arbitrary points of the interval $x_i\in(a,b),i=1,\ldots,N$, and for any positive weights

$$p_i\geq 0 \quad \text{for } i=1,\ldots,N, \quad \sum_{i=1}^{N} p_i=1 , \tag{A1}$$

the following inequality holds:

$$\mathcal{L}\left[\sum_{i=1}^{N} x_i p_i\right]\leq \sum_{i=1}^{N}\mathcal{L}(x_i)p_i . \tag{A2}$$

Theorem 2: Jensen's inequality in continuous form. If function $\mathcal{L}$: $\mathbb{R}\to\mathbb{R}$ is convex and continuous on the interval (a,b) and x: $\mathbb{R}\to\mathbb{R}$ such that $x(\rho)\in(a,b)$ if $\rho\in[r_1,r_2]$, then for a positive weight function $w(\rho)$,

$$w(\rho)\geq 0 \quad \text{for } \rho\in[r_1,r_2], \quad \int_{r_1}^{r_2} w(\rho)d\rho=1 , \tag{A3}$$

the following inequality holds:

$$\mathcal{L}\left[\int_{r_1}^{r_2} x(\rho)w(\rho)d\rho\right]\leq \int_{r_1}^{r_2}\mathcal{L}(x(\rho))w(\rho)d\rho . \tag{A4}$$

In the following considerations we will utilize the fact that $\mathcal{L}(x)=-\ln(x)$ is convex and continuous in the interval $(0,\infty)$.

For a finite lattice it is easy to verify using (2.1) that acting $p_i=Q_i$, $x_i=Q_i$ satisfies the conditions required by the finite form of Jensen's inequality. According to definitions (2.2) and (2.7), (A2) results in

$$\ln D\leq S . \tag{A5}$$

Similarly, $p_i=Q_i$, $x_i=1/Q_i$ satisfy again the required relations. In this case (A2) is equivalent to

$$S\leq \ln N . \tag{A6}$$

Subtracting $\ln D$ from inequalities (A5) and (A6), one easily arrives at

$$0\leq S_{\rm str}\leq -\ln q , \tag{A7}$$

which is exactly our basic inequality (2.10b).

For the continuous lattice model the range of integration $[r_1,r_2]$ is chosen as $[0,z]$, whereas $w(\rho)=f(\rho)\rho^{d-1}/F(z)$ plays the role of the weight function, which, according to definition (3.5b) of $F(z)$, satisfies (A3). First setting $x(\rho)=f(\rho)$, the corresponding form of (A4) is

$$-\ln\frac{G(z)}{F(z)}\leq\frac{H(z)}{F(z)} , \tag{A8}$$

which is equivalent to

$$0\leq S_{\rm str}(z) , \tag{A9}$$

where we have used expressions (3.5) and (3.7b). On the other hand, setting $x(\rho)=1/f(\rho)$ (A4) gives

$$-\ln\frac{E(z)}{F(z)}\leq-\frac{H(z)}{F(z)} . \tag{A10}$$

Subtracting $\ln[G(z)/F(z)]$ from both sides and utilizing Eqs. (3.7), one arrives at

$$S_{\rm str}(z)\leq -\ln q(z) . \tag{A11}$$

Inequalities (A9) and (A11) give the required relation (3.8b) for the structural entropy in the continuous lattice model.

In order to prove (3.8a) the range of integration will be chosen as above $[0,z]$, but with the weight function replaced by $w(\rho)=\rho^{d-1}/E(z)$. Since the function $\mathcal{L}(x)=x^2$ is convex and continuous in the interval $(0,\infty)$, application of Jensen's inequality (A4) with $x(\rho)=f(\rho)$, as well as definitions (3.5), result in

$$\left[\frac{F(z)}{E(z)}\right]^2 \leq \frac{G(z)}{E(z)} , \tag{A12}$$

which, considering expressions (3.7a) and (3.2b), is equivalent to (3.8a).

APPENDIX B: COMPLETENESS OF THE ALLOWED DOMAIN

The aim of this appendix is to prove that the allowed domain of the localization diagram

$$0<q\leq 1, \quad 0\leq S_{\rm str}\leq -\ln q \tag{B1}$$

is dense in the sense that for any pair $(\bar{q},\bar{S}_{\rm str})$ satisfying (B1) there exist a finite lattice and a wave function with actual localization quantities $(q,S_{\rm str})$ which approximate arbitrarily the values chosen originally.

This wave function can be constructed with a steplike charge distribution

$$Q_i=\begin{cases} Q_l & \text{for } i=1,\ldots,K, \\ Q_s & \text{for } i=K+1,\ldots,N \end{cases} \tag{B2}$$

on an N-site lattice, where for the "small" and "large" components $Q_s\leq Q_l$. Introducing

$$x=K/N, \quad l=Q_lN, \quad s=Q_sN , \tag{B3}$$

and using definitions (2.2), (2.3), (2.7), and (2.9), one easily gets for the normalization constraint (2.1b), filling factor and structural entropy,

$$1=(1-x)s+xl , \tag{B4a}$$

$$1/q=A=(1-x)s^2+xl^2 , \tag{B4b}$$

$$(-\ln q)-S_{\rm str}=B=(1-x)s\ln s+xl\ln l . \tag{B4c}$$

Substituting the required values $\bar{q}$ and $\bar{S}_{\rm str}$ into the left-hand side of (B4b) and (B4c), the task of finding a wave function with the proper localization quantities is equivalent to the determination of the roots x,l,s of the system of equations (B4), where $A=1/\bar{q}$, $B=(-\ln\bar{q})-\bar{S}_{\rm str}$, which according to (B1) satisfy

$$1\leq A, \quad 0\leq B\leq \ln A . \tag{B5}$$

The solutions of (B4) must fulfill the requirements

$$0\leq s\leq l, \quad 0\leq x\leq 1 \quad (x \text{ is rational}) . \tag{B6}$$

Equations (B4a) and (B4b), and restrictions (B6), lead to the proper solutions

$$l(x)=1+\left[\frac{1-x}{x}(A-1)\right]^{1/2} ,$$
$$s(x)=1-\left[\frac{x}{1-x}(A-1)\right]^{1/2} \tag{B7}$$

if $0<x\leq 1/A$. By substitution of (B7) into Eq. (B4c) the right-hand side can be written as

$$\mathcal{R}(x)\equiv\begin{cases} (1-x)s(x)\ln s(x)+xl(x)\ln l(x) \\ \qquad \text{if } x\in(0,1/A) , \\ 0 \quad \text{if } x=0, \\ \ln A \quad \text{if } x=1/A . \end{cases} \tag{B8}$$

Since $\mathcal{R}$ is continuous on the interval $[0,1/A]$, from the *Darboux property* [46] it follows that for any number B in the interval $[0,\ln A]$ there exists at least one $\bar{x}\in[0,1/A]$, such that $\mathcal{R}(\bar{x})=B$. If this $\bar{x}$ is a rational number, we have found in this way a charge distribution (B2) for which the localization quantities are exactly the required $(\bar{q},\bar{S}_{\rm str})$ values. If $\bar{x}$ is irrational, we can find arbitrarily close to it a rational number x', such that for the localization quantities of the generated charge distribution, $q'=\bar{q}$ and $|S'_{\rm str}-\bar{S}_{\rm str}|$ is arbitrarily small.

APPENDIX C: EXPLICIT FUNCTIONS FOR DIFFERENT KINDS OF DECAY FORM FUNCTION AND POLYNOMIAL FITS TO SOME $S_{\rm str}$ VERSUS q CURVES

In this appendix we will give the explicit form of $S_{\rm str}(z)$ and $q(z)$ for some decay form functions commonly appearing in various fields of physics. Once $S_{\rm str}(z)$ and $q(z)$ are obtained it is possible to draw the $S_{\rm str}(q)$ curves running over all the values of z, namely, $0\leq z<\infty$. We are going to apply Eqs. (3.7) based on definitions (3.5). In what follows $E(z)=z^d/d$ is used for all decay form functions. Some of these formulas may be somewhat complicated; therefore we will also give a usable polynomial fit to some curves $S_{\rm str}$ versus q.

1. Exponential decay

For the case of an exponential decay $f(\rho)=\exp(-\rho)$ we have $F(z)=\gamma(d,z)$, $G(z)=2^{-d}\gamma(d,2z)$, $H(z)=\gamma(d+1,z)$, where $\gamma(a,x)$ is the incomplete gamma function [47]

$$\gamma(a,x)=\int_0^x t^{a-1}e^{-t}dt . \tag{C1}$$

Using Eqs. (3.7) we obtain

$$q(z)=\frac{d2^d}{z^d}\frac{[\gamma(d,z)]^2}{\gamma(d,2z)} \tag{C2}$$

and

$$S_{\rm str}(z)=\frac{\gamma(d+1,z)}{\gamma(d,z)}-\ln\frac{\gamma(d,z)}{\gamma(d,2z)}-d\ln 2 . \tag{C3}$$

With the help of the relation $\gamma(d+1,z)=d\gamma(d,z)-z^de^{-z}$, one can easily show the validity of the $z\to 0$ limit of Eqs. (4.5) for extreme delocalization, and

$$\lim_{z\to\infty} q(z)=0, \quad \lim_{z\to\infty} S_{\rm str}(z)=d(1-\ln 2) \tag{C4}$$

for extreme localization (see also Sec. V).

2. Gaussian decay

The application of a Gaussian DFF $f(\rho)=\exp(-\rho^2)$ yields the integrals $F(z)=\beta(d,z)$, $G(z)=2^{-d/2}\beta(d,\sqrt{2}z)$,

$H(z)=\beta(d+2,z)$, where $\beta(a,x)$ is defined the following way:

$$\beta(a,x)=\int_0^x t^{a-1}e^{-t^2}dt \ . \tag{C5}$$

For even values of a ($a\geq 2$) this function is related to the incomplete γ functions $\beta(a,x)=\frac{1}{2}\gamma(a/2,x^2)$. For odd values of a ($a\geq 3$), $\beta(a,x)$ may be derived by partial integration with the help of $\beta(1,x)=(\sqrt{\pi}/2)\Phi(x)$, where $\Phi(x)$ is the error function. A straightforward calculation yields

$$q(z)=\frac{d(\sqrt{2})^d}{z^d}\frac{[\beta(d,z)]^2}{\beta(d,\sqrt{2}z)} \ , \tag{C6}$$

and

$$S_{\rm str}(z)=\frac{\beta(d+2,z)}{\beta(d,z)}-\ln\frac{\beta(d,z)}{\beta(d,\sqrt{2}z)}-\frac{d}{2}\ln 2 \ . \tag{C7}$$

These equations fulfill relation (4.5) for the case of extreme delocalization ($z\to 0$), and for extreme localization we get

$$\lim_{z\to\infty} q(z)=0, \quad \lim_{z\to\infty} S_{\rm str}(z)=\frac{d}{2}(1-\ln 2) \ . \tag{C8}$$

We have to point out that, due to the relation $\beta(2,x)=\gamma(1,x^2)/2$, we obtain identically the same curves $S_{\rm str}$ versus q for a two-dimensional Gaussian decay and a one-dimensional exponential decay.

3. Power-law decay

Here we give the explicit results for $f(\rho)=(1+\rho)^{-m}$, where $m>0$. The choice of this functional form of DFF is due to the requirements (3.2) and the asymptotic behavior $f(\rho)\to\rho^{-m}$. We give the explicit $F(z,m,d)$, $G(z,m,d)$, and $H(z,m,d)$ functions for the case when dimension d is an integer; however, it is straightforward to calculate these functions for noninteger values of d, i.e., for fractals:

$$F(z,m,d)=\int_0^z x^{d-1}(1+x)^{-m}dx=\sum_{k=0}^{d-1}\binom{d-1}{k}(-1)^k\frac{(1+z)^{d-k-m}-1}{d-k-m} \ , \tag{C9a}$$

$$G(z,m,d)=\int_0^z x^{d-1}(1+x)^{-2m}dx=F(z,2m,d) \ , \tag{C9b}$$

$$H(z,m,d)=m\int_0^z x^{d-1}(1+x)^{-m}\ln(1+x)dx$$
$$=\sum_{k=0}^{d-1}\binom{d-1}{k}(-1)^k\frac{m}{d-k-m}\left\{(1+z)^{d-k-m}\left[\ln(1+z)-\frac{1}{d-k-m}\right]+\frac{1}{d-k-m}\right\} \ . \tag{C9c}$$

For integers $m\leq d$ the functions in Eqs. (C9) have a different form. In what follows we give these exceptions for $F(z,m,d)$ and $H(z,m,d)$, keeping Eq. (C9b) in mind. Therefore, in $d=1$,

$$F(z,1,1)=\ln(1+z) \ , \tag{C10a}$$

$$H(z,1,1)=\tfrac{1}{2}[\ln(1+z)]^2 \ ; \tag{C10b}$$

in $d=2$,

$$F(z,1,2)=z-\ln(1+z) \ , \tag{C11a}$$

$$F(z,2,2)=\ln(1+z)-\frac{z}{1+z} \ , \tag{C11b}$$

$$H(z,1,2)=(1+z)\ln(1+z)-z-\tfrac{1}{2}[\ln(1+z)]^2 \ , \tag{C11c}$$

$$H(z,2,2)=[\ln(1+z)]^2-\frac{2}{1+z}[z-\ln(1+z)] \ ; \tag{C11d}$$

and in $d=3$,

$$F(z,1,3)=\ln(1+z)+\frac{z(z-2)}{2} \ , \tag{C12a}$$

$$F(z,2,3)=\frac{z(z+2)}{z+1}-2\ln(1+z) \ , \tag{C12b}$$

$$F(z,3,3)=\ln(1+z)+\frac{4z+3}{2(z+1)^2}-\frac{3}{2} \ , \tag{C12c}$$

$$H(z,1,3)=\tfrac{1}{2}[\ln(1+z)]^2+\tfrac{1}{2}(z-2)(z+1)\ln(1+z)$$
$$-\tfrac{1}{4}z(z-6) \ , \tag{C12d}$$

$$H(z,2,3)=\frac{2z}{1+z}[(z+2)\ln(1+z)-z]-2[\ln(1+z)]^2 \ , \tag{C12e}$$

$$H(z,3,3)=\frac{3}{4(1+z)^2}[2(4z+3)\ln(1+z)-z(7z+6)]$$
$$+\tfrac{3}{2}[\ln(1+z)]^2 \ . \tag{C12f}$$

Using formulas (3.7) the calculation of $q(z)$ and $S_{\rm str}(z)$ is straightforward. For any m and d it is also possible to show that the filling factor and the structural entropy obey relations (4.5) for extreme delocalization $z\to 0$. The limit of strong localization is complicated. Let us introduce the notation $q^\infty(m)=\lim_{z\to\infty}q(m,z)$ and $S^\infty_{\rm str}(m)=\lim_{z\to\infty}S_{\rm str}(m,z)$. In any dimension d for m obeying the relation $0<m<d/2$ one finds that $0<q^\infty(m)<1$ and $0<S^\infty_{\rm str}(m)<-\ln q^\infty(m)$. For $d/2\leq m\leq d$, one gets $q^\infty(m)=0$ and $S^\infty_{\rm str}(m)=\infty$; and for $m>d$, we have $q^\infty(m)=0$ and $0<S^\infty_{\rm str}(m)<\infty$. In the latter case we find that, for $m\to\infty$, $S^\infty_{\rm str}(m)\to d(1-\ln 2)$, as one would expect, since the power-law decay with $m\to\infty$ should show properties similar to those of the exponential decay.

4. Polynomial fits for the $S_{\rm str}$ versus q curves for exponential and Gaussian DFF

Since the computer programming of incomplete gamma functions $\gamma(a,x)$, as well as function $\beta(a,x)$, appearing in formulas (C2) and (C3), and (C6) and (C7), is rather

TABLE I. Coefficients of the eighth-order polynomial fits for Gaussian and exponential DFF and $d=1,2,3$. The ϵ_0 stands for the sum of residuals and ϵ_1 and ϵ_2 give the error of conditions, Eq. (C13). Note that the polynomial for $d=1$ and exponential DFF is identical to the one for $d=2$ and Gaussian DFF. The numbers in brackets indicate a multiplicative power of 10.

	Gaussian			Exponential	
Coeff.	$d=1$	$d=2$	$d=3$	$d=2$	$d=3$
c_0	0.1534	0.3068	0.4602	0.6137	0.9205
c_1	−0.0205	0.0191	−0.0660	0.0866	0.1631
c_2	0.5220	−0.6721	2.0374	−1.0719	−16.2938
c_3	−4.4657	7.4938	−18.5204	−13.4191	80.7179
c_4	17.3965	−34.7848	54.1223	65.7823	−216.7032
c_5	−33.7736	71.5218	−84.4764	−135.6169	344.7687
c_6	32.8366	−76.2570	75.6981	147.7381	−322.2612
c_7	−15.3259	41.5624	−36.7988	−83.2435	163.1958
c_8	2.6771	−9.1901	7.5435	19.1307	−34.5079
ϵ_0	1.38[−04]	9.80[−05]	1.61[−04]	4.23[−04]	6.58[−04]
ϵ_1	3.27[−11]	1.18[−10]	3.43[−10]	1.54[−10]	4.12[−10]
ϵ_2	9.16[−10]	5.94[−10]	9.58[−10]	2.08[−09]	3.19[−09]

complicated; we give here polynomial fits for the $S_{\rm str}(q)$ curves in these cases. For power-law decay, however, formulas (C9)–(C12) can be programmed easily.

We have fitted eighth-order polynomials fulfilling the following constraints [see Eqs. (C4), (C8), and (4.6)]:

$$\lim_{q\to 1} S_{\rm str}(q)=0, \quad \lim_{q\to 1}\frac{d}{dq}S_{\rm str}(q)=-\tfrac{1}{2}\ , \tag{C13}$$

and

$$\lim_{q\to 0} S_{\rm str}(q)=\begin{cases} d(1-\ln 2) & \text{for exponential DFF,} \\ \dfrac{d}{2}(1-\ln 2) & \text{for Gaussian DFF .} \end{cases} \tag{C14}$$

We have calculated $S_{\rm str}$ for 1000 equidistant q values ranging from 0 to 1 and fitted the polynomial of the form

$$S_{\rm str}(q)=\sum_{k=0}^{8} c_k q^k \tag{C15}$$

with a least-squares method. The coefficients of the fitted polynomials are listed in Table I. The value of ϵ_0 stands for the sum of the residuals, and ϵ_1 and ϵ_2 give the errors of conditions (C13) respectively. According to the overall statistics the error of the curves was $\epsilon_0\approx 10^{-4}$, and conditions (C13) were satisfied with an error of $\epsilon_{1,2}\approx 10^{-10}$.

APPENDIX D: CLM IN THE EXTREME DELOCALIZATION LIMIT

We will study here the behavior of the expression (3.7) for q and $S_{\rm str}$, as well as the slope of the $q\mapsto S_{\rm str}$ curve at the $z=R/\lambda\to 0$ limit.

We apply the first mean-value theorem of integral calculus [48] for the functionals (3.5). In accordance with the theorem there exist numbers ρ_F, ρ_G and ρ_H such that

$$F(z)=f(\rho_F)E(z), \quad \rho_F\in[0,z] \tag{D1a}$$

$$G(z)=f^2(\rho_G)E(z), \quad \rho_G\in[0,z] \tag{D1b}$$

$$H(z)=-f(\rho_H)\ln f(\rho_H)E(z), \quad \rho_H\in[0,z]\ . \tag{D1c}$$

Using (3.7) and the above formulas,

$$\lim_{z\to 0} q(z)=\lim_{z\to 0}\frac{f^2(\rho_F)}{f^2(\rho_G)} \tag{D2a}$$

and

$$\lim_{z\to 0} S_{\rm str}(z)=\lim_{z\to 0}\left[-\frac{f(\rho_H)\ln f(\rho_H)}{f(\rho_F)}+\ln\frac{f^2(\rho_G)}{f(\rho_F)}\right]. \tag{D2b}$$

Considering that all ρ_F, ρ_G, and ρ_H are in the interval $[0,z]$,

$$\lim_{z\to 0}\rho_F=\lim_{z\to 0}\rho_G=\lim_{z\to 0}\rho_H=0\ , \tag{D3}$$

from which, together with Eq. (3.2a), it follows that

$$\lim_{z\to 0} f(\rho_F)=\lim_{z\to 0} f(\rho_G)=\lim_{z\to 0} f(\rho_H)=1\ . \tag{D4}$$

Equations (D2) and (D4) imply the final result,

$$\lim_{z\to 0} q(z)=1, \quad \lim_{z\to 0} S_{\rm str}(z)=0\ . \tag{D5}$$

The slope of the $q\mapsto S_{\rm str}$ curve at the completely delocalized point $z=0$, $q=1$, $S_{\rm str}=0$ is

$$\alpha=\lim_{q\to 1}\frac{dS_{\rm str}}{dq}=\lim_{z\to 0}\frac{S'_{\rm str}}{q'}\ , \tag{D6}$$

where the prime means the first derivative with respect to variable z. Using definitions (3.7), straightforward calculation results in

$$\frac{S'_{\rm str}}{q'}=\frac{G/E}{(F/E)^3}\,\frac{-(G/E)(F/E+H/E)F'+(F/E)^2G'+(F/E)(G/E)H'}{-(F/E)(G/E)E'+2(G/E)F'-(F/E)G'}\ . \tag{D7}$$

Substituting now expressions (D1) and taking into account limits (D4) one arrives at

$$\alpha=\lim_{z\to 0}\frac{-F'+G'+H'}{-E'+2F'-G'}\ . \tag{D8}$$

Calculation of the appropriate derivatives from the explicit formulas (3.5) leads to

$$\alpha=\lim_{z\to 0}\frac{f(z)[\ln f(z)-f(z)+1]}{[f(z)-1]^2}$$
$$=\lim_{f\to 1}\frac{f(\ln f-f+1)}{(f-1)^2}\ . \tag{D9}$$

Two consecutive applications of L'Hospital's rule to the second expression of (D9) give the final result $\alpha=-\frac{1}{2}$.

APPENDIX E: RELATIONS AMONG LOCALIZATION CLASSES

In this appendix we will investigate the various relations among the localization classes L_d, L_f, L_n, and L_s. In the following considerations it will be useful to refer to the following inequality. For nonexploding decay form functions, relations (3.2) and definitions (3.5) result in

$$0<G(z)\le F(z)\le E(z)\quad \text{for } 0<z<\infty\ . \tag{E1}$$

Let us prove first the equivalence of the classes L_n and L_s. If $f\in L_n$, (5.5) and (E1) lead to

$$0<\lim_{z\to\infty}G(z)\le\lim_{z\to\infty}F(z)<\infty\ . \tag{E2}$$

As according to (3.6b) and (3.6c),

$$D(z)=ns_d\lambda^d F^2(z)/G(z)\ , \tag{E3}$$

(E2) shows that for a given λ limit (5.4) is finite; thus $f\in L_s$. We will give an indirect proof for the opposite statement, supposing that there exists a finite-sized function f (5.4) but $\lim_{z\to\infty}F(z)=\infty$. Considering (E3) this is possible only if $\lim_{z\to\infty}G(z)=\infty$, as well. Applying now L'Hospital's rule, as well as (3.5), one arrives at

$$\lim_{z\to\infty}D(z)=2ns_d\lambda^d\lim_{z\to\infty}F(z)/f(z)\ , \tag{E4}$$

which must be infinite by our assumption $\lim_{z\to\infty}F(z)=\infty$ and (3.2). This is a contradiction; thus $f\in L_s$ implies $f\in L_n$, i.e., $L_s\equiv L_n$.

Next we will show that *norm localization* indicates *filling localization*, $L_f\supseteq L_n$. We have seen previously in (E2) that if $f\in L_n$ both $\lim_{z\to\infty}F(z)$ and $\lim_{z\to\infty}G(z)$ are finite, while the explicit form (3.5a) shows $\lim_{z\to\infty}E(z)=\infty$. Using definition (3.7a) for q we get $\lim_{z\to\infty}q(z)=0$, or $f\in L_f$.

On the other hand, all *filling localized* functions are *decay localized* at the same time, $L_d\supseteq L_f$. In order to prove this statement we can treat two subcases. First, if f is not only *filling localized* but *norm localized,* too, the convergence of the norm integral $F(z)$ requires $\lim_{z\to\infty}f(z)=0$. In the second case, $\lim_{z\to\infty}F(z)=\infty$, but since $f\in L_f$, $\lim_{z\to\infty}q(z)=0$. Using now definition (3.7a) and inequalities (E1) one can conclude that $F(z)/G(z)\ge 1$ and $\lim_{z\to\infty}q(z)=0$ requires

$$\lim_{z\to\infty}F(z)/E(z)=0\ . \tag{E5}$$

L'Hospital's rule shows again that

$$\lim_{z\to\infty}F(z)/E(z)=\lim_{z\to\infty}f(z)=0\ , \tag{E6}$$

i.e., $f\in L_d$.

From the above considerations it is clear now that $L_d\supseteq L_f\supseteq L_n\equiv L_s$, but it is also possible to see that the containment relations are strict, i.e.,

$$L_d\supset L_f\supset L_n\ . \tag{E7}$$

The counterexample $f(z)=1/(1+z)$ in dimension $d=3$ is *decay localized* but neither *filling localized* nor *norm localized.* The same function in dimensions $d=2$ and $d=1$ is both *decay localized* and *filling localized* at the same time, but does not belong to the class of normalizable functions L_n. The proof is straightforward, considering the asymptotic behavior of functions $E(z)$, $F(z)$, and $G(z)$.

[1] P. W. Anderson, Phys. Rev. **109**, 1402 (1958).
[2] D. J. Thouless, Phys. Rep. C **13**, 93 (1974).
[3] *Anderson Localization,* edited by Y. Nagaoka and H. Fukuyama (Springer, Berlin, 1982).
[4] *Localization, Interaction and Transport Phenomena,* edited by B. Kramer, G. Bergmann, and Y. Bruynseraede (Springer, Berlin, 1984).
[5] D. G. Bergmann, Phys. Rep. **107**, 1 (1984).
[6] P. A. Lee and T. V. Ramakrishnan, Rev. Mod. Phys. **57**, 287 (1985).
[7] *Anderson Localization,* edited by T. Ando and H. Fukuyama (Springer, Berlin, 1988).
[8] E. Abrahams, P. W. Anderson, D. C. Licciardello, and T. V. Ramakrishnan, Phys. Rev. Lett. **42**, 673 (1979).
[9] W. T. Ching and D. L. Huber, Phys. Rev. B **25**, 1096 (1982); **26**, 5596 (1982).
[10] P. V. Elyutin, J. Phys. C **16**, 4151 (1983).
[11] A. Blumen, J. P. Lemaistre, and I. Mathlouthi, J. Chem. Phys. **81**, 4610 (1984).
[12] Zheng Zhaobo, J. Phys. C **20**, 4627 (1987); **21**, 1753 (1988).
[13] M. K. Gibbon, D. E. Logan, and P. A. Madden, Phys. Rev. B **38**, 7292 (1988).
[14] D. Weaire and A. R. Williams, J. Phys. C **9**, L461 (1976); **10**, 1239 (1976); D. Weaire and V. Srivastava, *ibid.* **10**, 4309 (1977).
[15] D. Würtz, T. Schneider, A. Politi, and M. Zannetti, Phys. Rev. B **39**, 7829 (1989).
[16] P. de Vries, H. De Raedt, and A. Lagendijk, Phys. Rev. Lett. **62**, 2515 (1989).
[17] T. Fujiwara, M. Kohmoto, and T. Tokihiro, Phys. Rev. B **40**, 7413 (1989).
[18] Y. E. Lévy and B. Souillard, Europhys. Lett. **4**, 233 (1987); B. Souillard (unpublished).
[19] Y. Sasajima, T. Miura, M. Ichimura, M. Imabayashi, and B. Yamamoto, J. Phys. Condens. Matter **1**, 4755 (1989).
[20] G. Anathakrishna, J. Phys. Condens. Matter **2**, 1343

(1990); V. Kumar, J. Phys. Condens. Matter **2**, 1349 (1990).
[21] G. Casati, I. Guarneri, F. Izrailev, and R. Scharf, Phys. Rev. Lett. **64**, 5 (1990); G. Casati, L. Molinari, and F. Izrailev, *ibid.* **64**, 1851 (1990); F. M. Izrailev, J. Phys. A **22**, 865 (1989).
[22] C. M. Soukoulis, E. N. Economou, G. S. Grest, and M. H. Cohen, Phys. Rev. Lett. **62**, 575 (1989).
[23] D. H. Dunlap, K. Kundu, and Ph. Phillips, Phys. Rev. B **40**, 10 999 (1989). See also D. H. Dunlap and Ph. Phillips, J. Chem. Phys. **92**, 6093 (1990); D. H. Dunlap, H.-L. Wu, and Ph. Phillips, Phys. Rev. Lett. **65**, 88 (1990).
[24] Qin Li and D. J. Thouless, Phys. Rev. B **40**, 9738 (1989).
[25] T. Ando, Phys. Rev. B **40**, 5325 (1989); Prog. Theor. Phys. Suppl. **84**, 69 (1985).
[26] For a review, see R. F. W. Bader and T. T. Nguyen-Dang, Adv. Quantum Chem. **14**, 63 (1981); R. F. W. Bader, T. T. Nguyen-Dang, and Y. Tal, Rep. Progr. Phys. **44**, 893 (1981).
[27] R. J. Bell and P. Dean, Disc. Farad. Soc. **50**, 55 (1970).
[28] I. Varga (unpublished).
[29] J. Pipek, Int. J. Quantum Chem. **36**, 487 (1989).
[30] R. J. McEliece, *The Theory of Information and Coding,* Encyclopedia of Mathematics and its Applications Vol. 3 (Addison-Wesley, Reading, MA, 1977), p. 277.
[31] F. Yonezawa, J. Non-Cryst. Solids **35&36**, 29 (1980); R. Blümel and U. Smilansky, Phys. Rev. Lett. **52**, 137 (1984); Phys. Rev. A **30**, 1040 (1984); J. Pipek, Int. J. Quantum Chem. **27**, 527 (1985); J. Reichl, Europhys. Lett. **6**, 669 (1988); F. M. Izrailev, Phys. Lett. **134A**, 13 (1988).
[32] J. Pipek, I. Varga, and T. Nagy, Int. J. Quantum Chem. **37**, 529 (1990).
[33] I. Varga and J. Pipek, Phys. Rev. B **42**, 5335 (1990).
[34] T. A. Brody, J. Flores, J. B. French, P. A. Mello, A. Pandey, and S. S. M. Wong, Rev. Mod. Phys. **53**, 385 (1981).
[35] For a review, see J. B. Sokoloff, Phys. Rep. **126**, 189 (1985).
[36] S. Das Sarma, S. He, and X. C. Xie, Phys. Rev. Lett. **61**, 2144 (1989); Phys. Rev. B **41**, 5544 (1990).
[37] I. Varga, J. Pipek, and B. Vasvári, Phys. Rev. B **46**, 4978 (1992).
[38] J. Pipek, Int. J. Quantum Chem. **35**, 487 (1989).
[39] For recent reviews, see K. Jug, Int. J. Quantum Chem. **37**, 403 (1990); J. Sadley, *Semi-Empirical Methods of Quantum Chemistry* (Horwood, Chichester, 1985).
[40] J. N. Murrel and A. J. Hargett, *Semi-Empirical Self-Consistent-field Molecular-orbital Theory of Molecules* (Wiley-Interscience, London, 1972).
[41] M. H. McAdon and W. A. Goddard III, J. Chem. Phys. **88**, 277 (1988).
[42] Z. Q. Zhang and P. Sheng, Phys. Rev. Lett. **67**, 2541 (1991); R. Harris and A. Honari, Phys. Rev. B **42**, 7266 (1990).
[43] I. Varga and B. Vasvári, in *Proceedings of the 19th Symposium on Electronic Structure, Holzhau, 1989,* edited by P. Ziesche (Technische Universität Dresden, Dresden, 1989), p. 209.
[44] I. Varga and B. Vasvári (unpublished).
[45] A. M. Yayannavar and N. Kumar, Phys. Rev. B **37**, 573 (1988).
[46] K. Kuratowski, *Introduction to Calculus* (Pergamon, Oxford, England, 1961), p. 111.
[47] *Handbook of Mathematical Functions,* edited by M. Abramowitz and I. A. Stegun (Dover Publications, New York, 1968), p. 260.
[48] K. Kuratowski, *Introduction to Calculus,* Ref. [46], p. 253.